The Passive Response of Skeletal Muscle to Compressive Impact Loading

Michael Takaza[1], Ciaran K. Simms[2]

Abstract

Appropriate mechanical representation of passive muscle tissue is crucial for human body impact modelling. This requires an understanding of the deformation behaviour of the tissue. Existing data mostly relate to uniaxial compression tests at normalized strain rates of between 0.05%/s and 3200%/s and Split Hopkinson bar tests at normalized strain rates of above 54,000%/s. Thus data on fresh tissue in both the fibre and cross-fibre direction at normalized strain rates relevant to automotive accidents are needed. In this paper results of compressive loading of freshly slaughtered porcine muscle samples using a drop-tower testing rig are reported. Fibre and cross-fibre compression tests at strain rates varying from 11,600%/s to 37,800%/s were performed. Results show a nonlinear stress-stretch relationship as well as a clear rate dependency. The mean (standard deviation) engineering stress in the fibre direction at a stretch of 0.7 was 22.03kPa (1.5kPa) at a strain rate of 22,000%/s and 37.06kPa (3.0kPa) at 37,800%/s. For the cross-fibre direction, the equivalent engineering stresses were 5.95kPa (0.6kPa) at 11,600%/s, 25.88kPa (5.3kPa) at 22,000%/s and 43.68kPa (1.4kPa) at 37,800%/s. However, significant local strain variations and an average of 8% mass loss were observed, highlighting the difficulties in these kinds of tests.

Keywords

Muscle compression, impact loading, deformation behaviour

I. INTRODUCTION

Skeletal muscle accounts for about 40% of body mass [1, 2] and an understanding of its deformation properties is therefore very important for impact biomechanics research. However, the three dimensional compressive properties of fresh skeletal muscle at rates experienced during typical sports and automotive impacts are not well understood [3], and tissues tested after the onset of rigor mortis behave significantly differently [4].Therefore, although finite element human body models including muscle tissue are routinely used in impact biomechanics research, their utility remains limited mainly by uncertainties in the constitutive representation of the soft tissues. Accordingly, measuring the rate dependent compressive properties of skeletal muscle is an important research goal and is the focus of this paper.

Skeletal muscle is composed of about 70-80% water, 3% fat and 10% collagen [5]. It exhibits a fibre-oriented structure, with each muscle composed of fascicles containing bundles of fibres which themselves are composed of parallel bundles of myofibrils. There is a dense network of connective tissues which surrounds groups of fibres and this too has a hierarchical structure. Epimysium surrounds the whole muscle, perimysium surrounds bundles of muscle fibres and endomysium surrounds each muscle fibre individually. Arising from this structure, skeletal muscle presents a nonlinear elastic, non-homogeneous, anisotropic and viscoelastic behaviour [3, 4].

Tests on fresh animal tissue at very low strain rates (approx. 0.05%/s) have shown that the compressive stress response in skeletal muscle depends on the strain rate [6-10] and on the angle between the fibre orientation and the loading direction [4, 6, 11]. Van Sligtenhorst et al investigated the compressive behaviour of bovine skeletal muscle samples at 10%/s, 100000%/s, 1700s^{-1} and 230000%/s strain rates [10], and observed a stiffness response that was highly dependent on the applied strain rate. Dhaliwal et al performed high impact testing experiments using cadavers [12] and volunteer tests on the lower limb [12, 13] have been performed, but it was not possible to extract stress-strain data by this method.

[14] performed compressive impact tests but they used surgical scraps of human tissue which had been frozen and then thawed and the state of rigor mortis is unfortunately unknown in those tests. Furthermore, they tested only in the cross-fibre direction and did not report quasi-static results so that the evolution of strain rate effects cannot be readily assessed.

1. Michael Takaza is a PhD student in Soft Tissue Mechanics at Trinity College Dublin in Ireland. Email: takazam@tcd.ie Ph. +353 1 896 2978.
2. Dr. Ciaran Simms is an Assist Prof in the Department of Mechanical & Manufacturing Engineering and a PI in the Centre for Bioengineering at Trinity College Dublin, Ireland.

Overall, existing data on fresh tissue free from rigor mortis mostly relate to uniaxial compression tests (ramp or cyclic about a mean compression level) on animal tissue at normalized strain rates of between 0.05%/s and 3200%/s [4, 15] and split Hopkinson bar tests carried out in experiments with strain rates above 54,000%s-1 [8, 10].

For a typical vehicle frontal impact at 48km/h, soft tissue strain rates in the region of 25,000%/s may be expected [3], but comparable experimental data relating to the stress strain behaviour of fresh muscle tissue in both the fibre and cross-fibre direction at these rates are not available. Accordingly, this paper reports on experimental characterisation of the passive skeletal muscle mechanical properties in compression at strain rates corresponding to 11,600%s^{-1}, 22,000%s^{-1} and 37,800%s^{-1} using freshly harvested porcine tissue of a defined geometric shape. To achieve this, an instrumented custom-designed drop-tower testing rig was constructed to apply soft tissue deformation and measure deformation loads using high-speed video analysis of marker dots on the tissue.

II. METHODS

Experimental Rig

A custom rig was constructed to compress cuboid muscle samples (vertical height approximately 1cm) between two platens, see Fig. 1. The lower platen is stationary and connected to the base of the rig through a force transducer (PCB Piezotronics 208C04, see Fig. 2). The upper platen is connected to a falling mass plate to deliver dynamic deformation of the samples. The aluminium falling mass plate was designed to slide down two 10mm diameter parallel silver steel rods, which were held vertical and parallel by constructing a frame that maintained the rods in significant tension during testing. The falling mass plate slides over the silver steel rods via custom-made PTFE bearings. Bearing alignment plates were used to allow for fine-tuning (see Fig. 1). An accelerometer (PCB Piezotronics 353B03), see Fig. 2) was mounted on top of the falling mass plate to measure acceleration, see Fig. 1 and Fig. 2. A second force transducer (PCB Piezotronics 208C04) was mounted between the falling mass plate and the upper platen, see Fig. 2. The tissue specimens were placed on the bottom platen (Fig. 3).

The force transducers and the accelerometer were connected to a data acquisition PC and data were logged using Labview. A high speed camera (Mikrotron HiSpec) was used to capture specimen deformation. Labview was used to control and monitor the accelerometer signal and a rising edge signal was used to trigger data acquisition. The transducer signals were sampled at 25 kHz and the high speed video was sampled at 10KHz.

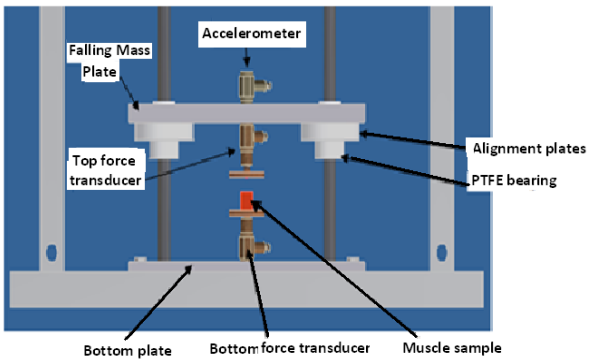

Figure 1. Schematic of the bottom part of the testing rig, the strain control plates are excluded for clarity.

The maximum compressive deformation was controlled by a strain control plate (Fig. 3), which allowed the gap between the platens to be adjusted to the maximum deformation required while preventing complete destruction of the samples. For the tests reported here, the gap was set at 50% of the sample height after which the falling mass plate struck the strain control plate. The design ensures the overall sample deformation rate is effectively constant between first contact of the falling mass plate with the tissue and contact of the falling mass plate with the strain control plate.

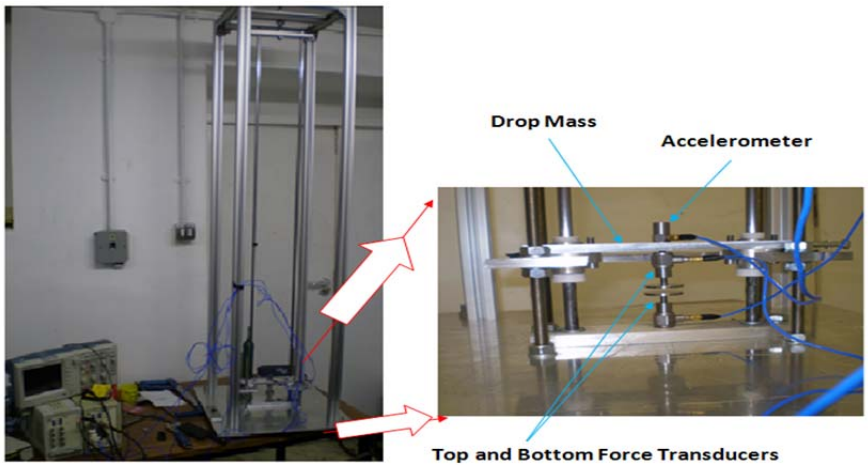

Figure 1. The drop tower testing rig with the bottom part where the tissue impact loading takes place magnified on the right image.

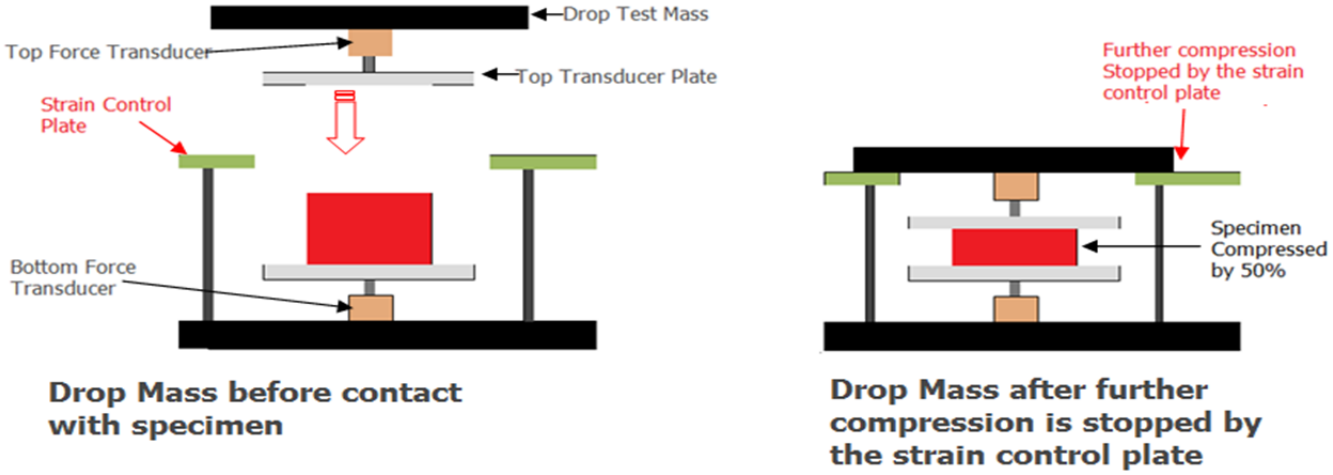

Figure 2. Drop test rig illustration, showing the strain control plate and how it controls the selected compression

Specimen Preparation

Freshly harvested porcine Longissimus dorsi samples were prepared from 3 month old pigs to produce approximately cuboid samples. Samples were compressed either in the cross-fibre (compression applied to face A or C) or the fibre direction (compression applied to face B), see Fig. 4a. The sample height for all tests was approximately 10mm and nominally cubic samples were used for the cross-fibre direction tests. For the fibre direction tests, the width and depth were set to approximately 20mm to reduce the buckling effects [4, 10, 16]. Producing cubic samples is very difficult given the very low stiffness of fresh skeletal muscle tissue. Testing was performed within 2 hours after the death of the animal to avoid the effects of rigor mortis [4].

Data Analysis

Each specimen was marked with 9 dots painted on a side face of the samples prior to testing (using a black fine line waterproof pen (Mitsibishi, Uni-ball eye) as shown in Fig. 4B. The deformation of the marker dots was then tracked using Matlab-based image analysis methods [17]. The strain for the overall deformation of the specimen was obtained using the platen displacement from the video data. For local deformations within the samples, the region of interest shown in Fig. 4B was divided into 6 sub-regions as labelled and the local stretch ratios (λ) were calculated by dividing the current height (L1) by the original height (L0):

$$\lambda = \frac{L_1}{L_0} \qquad (1)$$

Engineering stress (σ) is presented in favour of Cauchy stress , as the deformation was found to be not uniformly distributed from top to bottom, and this was found by dividing the force by the original cross-sectional area:

$$\sigma = \frac{F}{A_0} \quad (2)$$

where A_0 is the original area, and F is the current force.

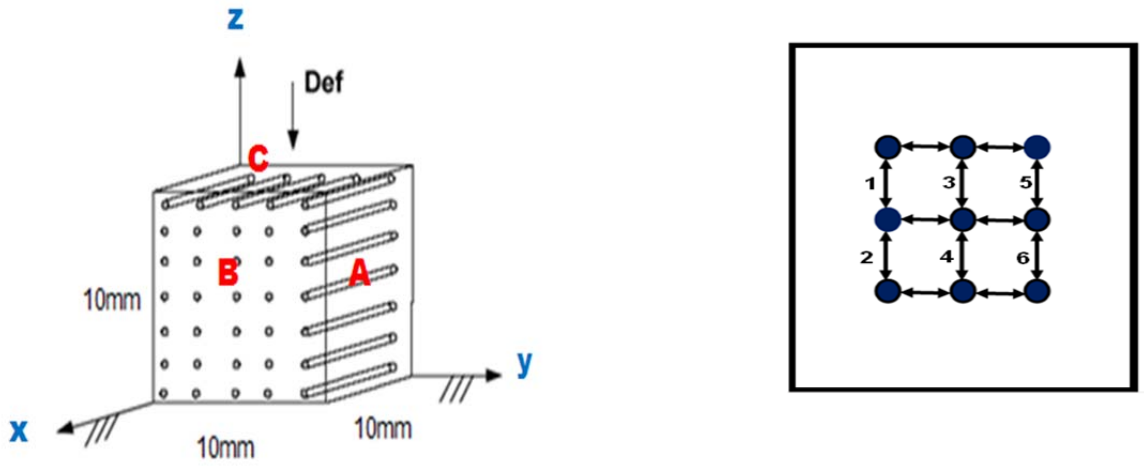

A ***B***

Figure 3A. Specimens illustrating the cross-fibre, fibre and 45 degrees to the fibre direction. The surfaces are marked A (cross-fibre direction), B (fibres direction) and C (cross-fibre direction). Fig. 4B shows schematic regions of interest used during image strain analysis.

Testing Matrix

A total of thirty one compressive impact tests were performed at different strain rates in the fibre and cross-fibre direction as shown in Table 1.

TABLE I
The tissue testing matrix

Testing Direction	Specimen Qty	Impact Velocity m/s	Avg Specimen height	Strain Rate %/s
Cross-Fibre	4	1.16	10.03 ± 0.21	11600
Cross-Fibre	12	2.2	9.78 ± 0.44	22000
Cross-Fibre	5	3.78	10.29 ± 0.36	37800
Fibre	5	2.2	20.23 ± 0.38	2200
Fibre	5	3.78	20.03 ± 0.44	37800

III. RESULTS

Due to the volume of data generated, typical results are shown in detail first and then a statistical description of the variability is presented. Analysis was carried out to verify that the applied strain rate is constant over the very small distances relevant to the sample compression. Fig. 5 shows that the platen displacement is effectively constant after tissue compression commences at approx. 1.1ms, thereby ensuring and effectively constant strain rate during the tests.

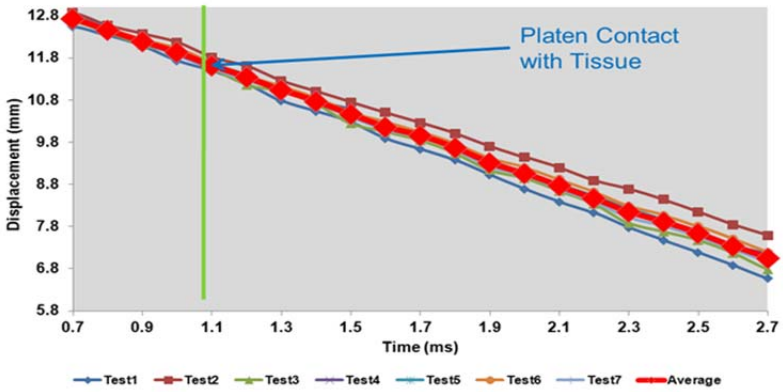

Figure 4: Upper compression platen displacement time history

Fig. 6 shows a typical time history sequence of the upper and lower force transducers and the applied load approximated using the accelerometer signal (unfiltered) by combining it with the mass of the falling plate. The upper force transducer curve presented is inertia-compensated to account for the mass of the upper platen. It can be seen that, up to the time of peak sample compression around 1.6ms, the three force estimates are very similar, which seems to show that the force is equilibrated throughout the sample during compression.

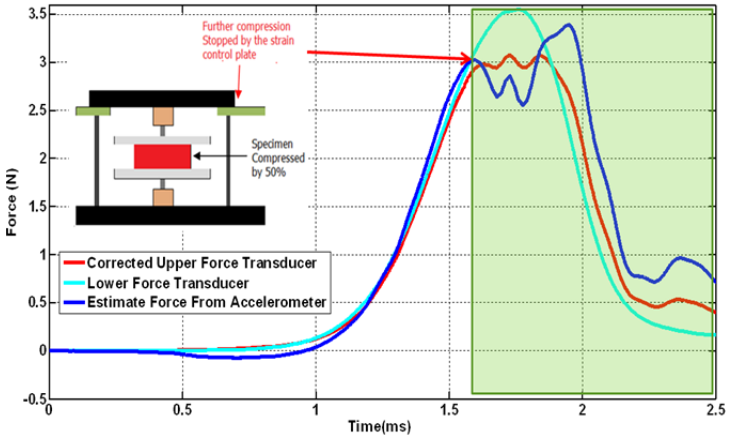

Figure 6. Typical accelerometer and force transducer results (the corrected upper transducer reading accounts for the platen inertia)

A typical cross-fibre direction specimen deformation during compression is presented in Fig. 7 (ie compression applied to cut face C in Fig 4A). The first row (R1) shows a camera view on a face perpendicular to the muscle fibres (face B in fig. 4A). The middle row (R2) shows a camera view on a face parallel to the muscle fibres (face A in fig. 4A). Since only one high speed camera was available, the first row and second row in Fig. 7 represent images from tests on different samples. The bottom row shows the capability of the Matlab code in tracking the marker centres initially (R3a) and at the end (R3b). The initial (red plus symbol) and final (blue circle symbol) marker locations are overlaid on the undeformed image in R3c.

Typical within-specimen strain variation for cross-fibre direction compression (compression applied to cut face C in Fig 4A) is shown in Fig. 8 and Fig. 9, with the strains found from tracking the dots located on a cut face perpendicular (surface B in Fig. 4A) and parallel (surface A in Fig. 4A) to the fibres respectively. Since each sample was tested only once, Fig. 8 and Fig. 9 represent tests on different samples. Assuming a uniform strain based on the platen displacement and a uniform stress distribution throughout the cross-section of the sample at each time point, nominal Stress-stretch ratio curves were derived for comparison with other published work, see Fig. 10 and Fig. 11 for the cross-fibre and fibre directions respectively.

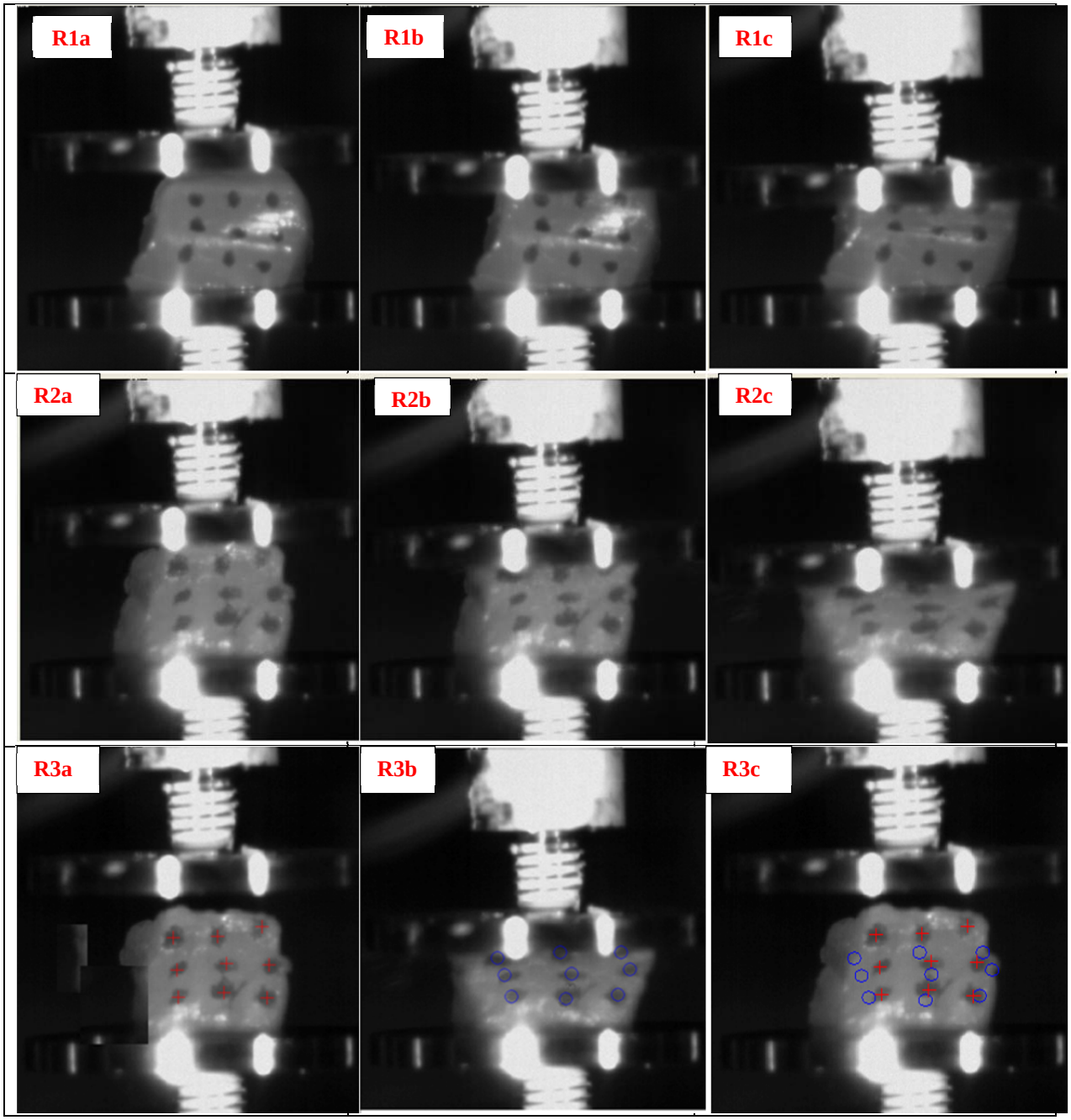

Figure 5. Sample deformation sequences. The first row (R1) shows the cross-fibre surface (marked B in fig. 4A) during the experimental testing. The middle row (R2) shows the cross-fibre surface (marked A in fig. 4A). The First row and second row came from different samples. The bottom row shows the capability of the Matlab code in finding the marker centres initially (R3a) and at the end (R3b). The initial and final marker locations are overlaid on the undeformed image in R3c.

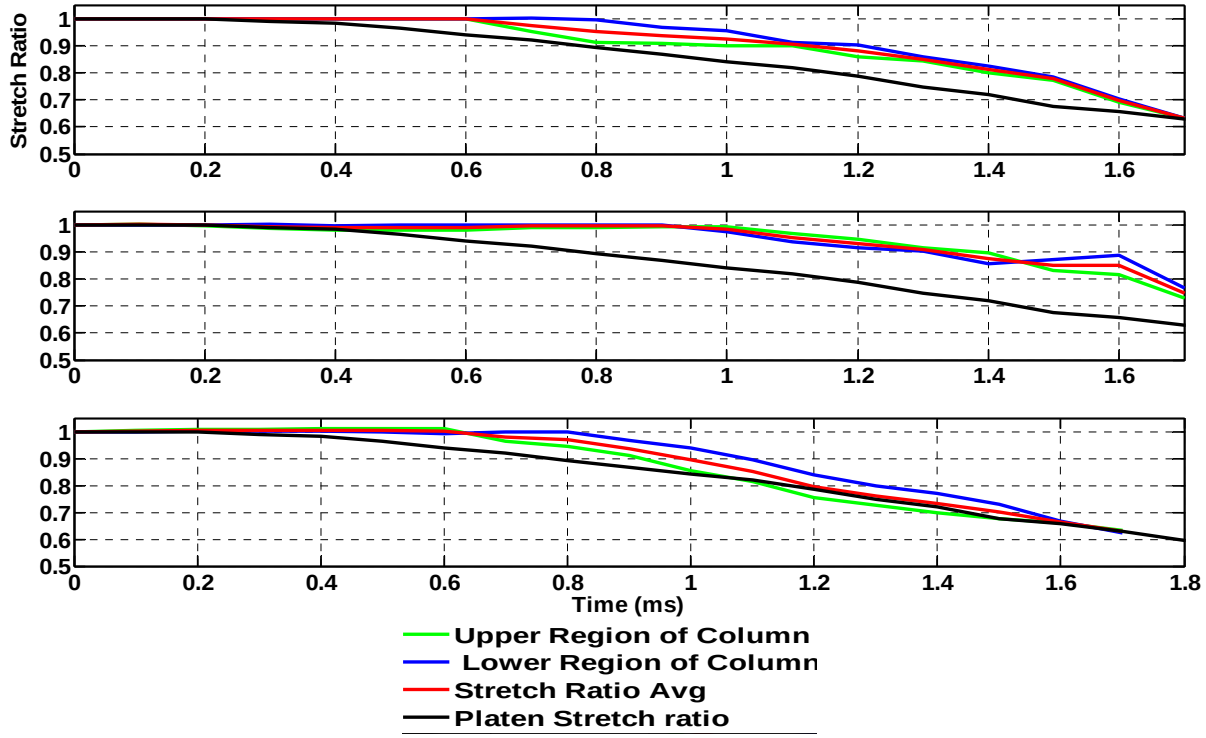

Figure 6. Typical strain variation within the regions of interest for cross-fibre direction testing. Rows 1 to 3 show the strain variation of the left, middle and right column (see Fig. 4B) respectively as observed from a cut face parallel to the muscle fibre direction (Marked as A in Fig.4A).

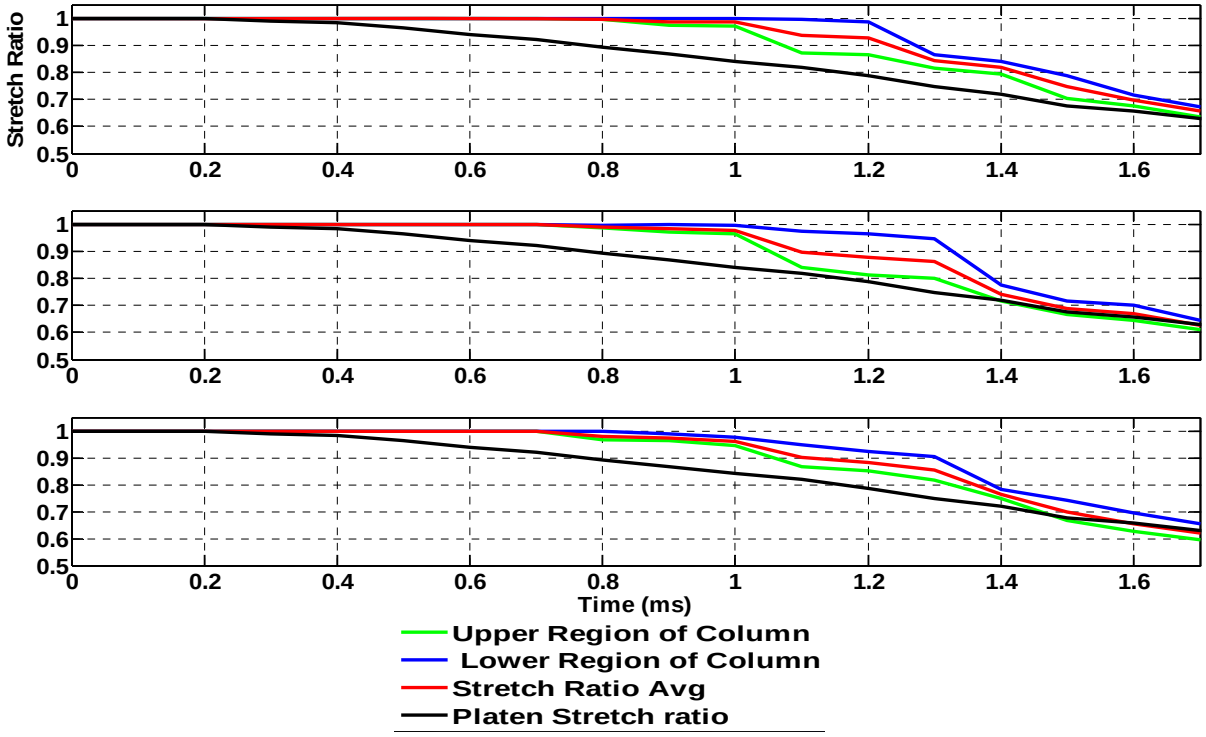

Figure 7. Typical strain variation within the regions of interest for cross-fibre direction testing. Rows 1 to 3 show the strain variation of the left, middle and right column (see Fig. 4B) respectively as observed from a cut face perpendicular to the muscle fibre direction (Marked as B in Fig.4A).

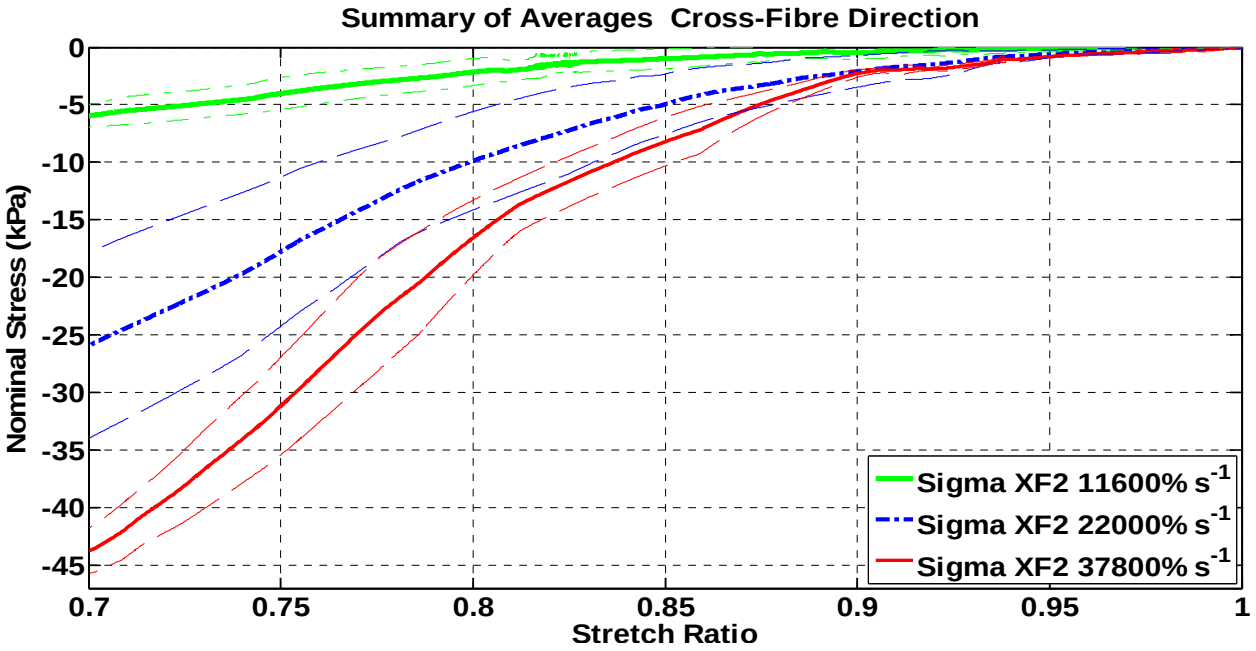

Figure 8: Nominal Stress-stretch ratio curves of the porcine skeletal muscle tissue for loading in the cross-fibre direction (ie when the loading is perpendicular to the fibre direction).

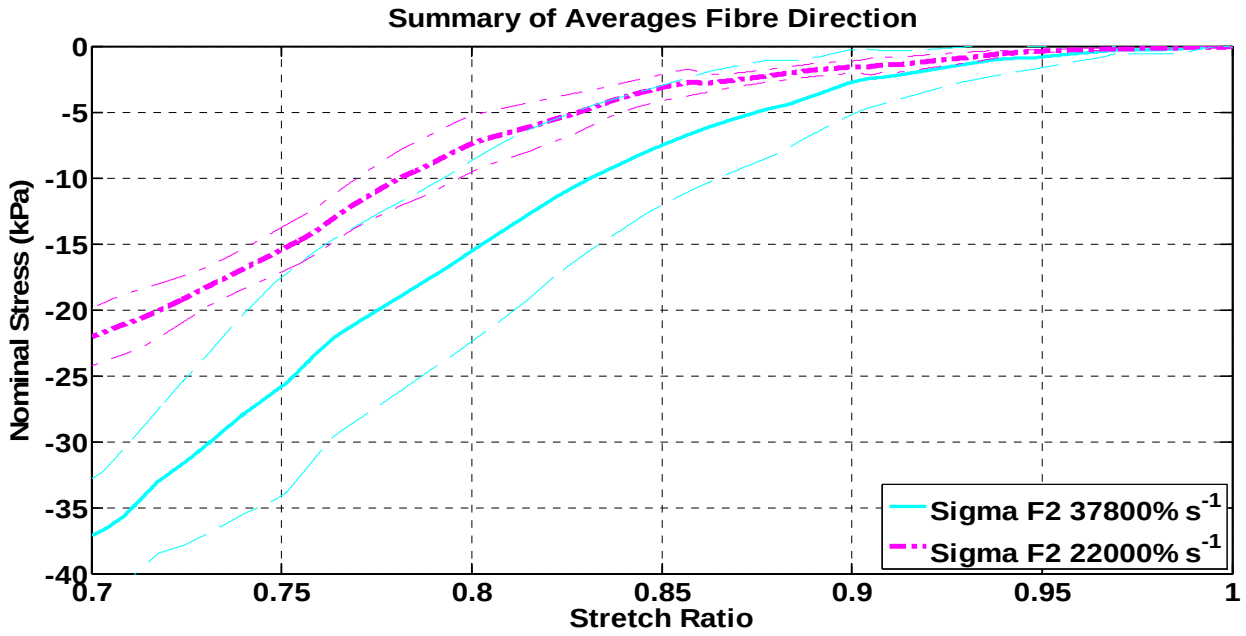

Figure 9: Nominal Stress-stretch ratio curves of the porcine skeletal muscle tissue in the fibre direction (ie when the loading is parallel to the muscle fibre direction).

IV. DISCUSSION

The goal of this work was to perform dynamic uniaxial compressive tests on uniformly shaped samples of freshly harvested skeletal muscle tissue in both the fibre and cross-fibre direction at rates relevant to automotive injuries. However, as can be seen from Fig 7 (R1a), preparation of uniform samples is difficult due to the extremely soft nature of the tissue which deformed significantly even under its own weight. Accordingly, Fig. 7 shows that some shearing as well as axial compression occurred during the sample deformation. This is the result of a number of factors including the difficulty in preparing cubic specimens, the interaction of the microstructural components of solid matrix and fluid and the impact nature of the applied deformation. These results are evident from the strain time histories in the different regions presented in Fig. 8 and Fig. 9. Nonetheless, these kinds of tests appear to be the closest we can get to pure uniaxial compression for these tissues.

The marker tracking software was found to successfully locate the displacement of the nine dots on the images, see Fig. 7 (R3), and this provided a reliable local strain measure. The resulting strain time history data presented for Fig. 8 and Fig. 9 are typical individual specimen results for cross-fibre direction impacts.

Fig. 8 shows the typical evolution of strain in the different regions of the sample as a function of time for the cross-fibre direction tests when viewed orthogonal to the muscle fibres (A in Fig 4A). It can be seen that the strain in the upper regions is initially greater than in the lower regions, but this equalizes towards the end of the test. Furthermore, the strain is greater at the left and right edges than in the middle of the sample. This may be because fluid expulsion is easier at the free edges, and the muscle fibres collapse earlier at these two edges. This could trap the fluid located at the specimen centre, unless it can pass through the connective tissue matrix, and this would be consistent with lower rate results obtained previously by our group [15], where the fluid expulsion appeared to be along rather than across the muscle fibres. The fluid mass loss was 8% on average during the testing.

Fig. 9 shows the equivalent results for a cross-fibre direction test when viewed parallel to the muscle fibres (B in Fig 4A). It is again evident that the strain is initially greater at the top of the sample than at the bottom, but now the strain at the left and right edges is similar to the strain in the middle of the sample. The result highlights the dependency of the strain on the chosen region (see Fig. 4B) and the results are significantly different to the stretch calculated from the platen displacements.

The speed of an elastic stress wave in a fluid is around 1500m/s [18, 19]. For the sample geometries used, this elastic stress wave would pass through the sample in microseconds and cannot be observed in the high speed video images (sample rate 10kHz), but it may be the reason why the upper and lower force time histories shown in Fig. 6 match well. A separate densification wave, where the tissue is seen to collapse, was observable at a much lower speed of approximately 10m/s and is evident in the strain time history in Fig 8 and Fig 9 and is shown schematically in Fig. 12.

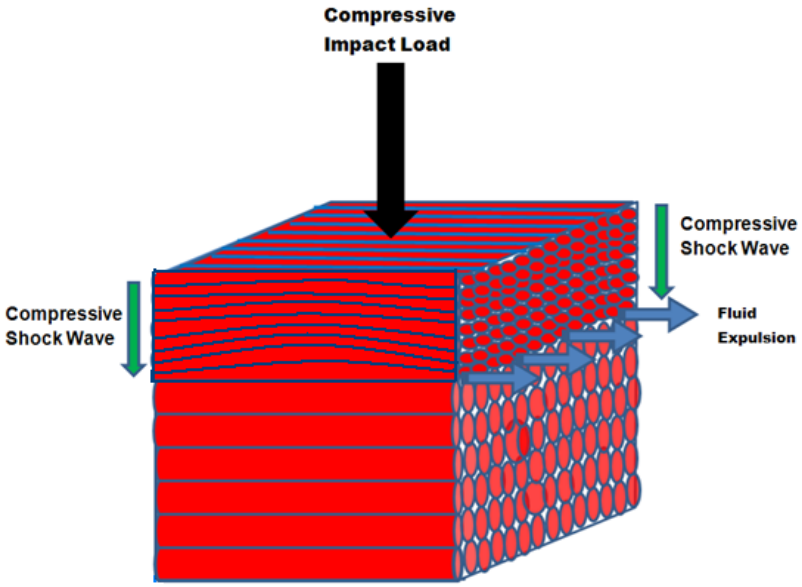

Figure 10. Schematic illustration of the strain process during impact loading

Given the observation that the tissue compression moves through the sample in a wave-like manner (the initial compression in the upper portions of the sample is greater than in the lower portions of the sample as shown in Fig. 8 and Fig 9), it is surprising that the load measured at the top and bottom of the sample appears to be substantially the same (when correcting for the inertia of the upper platen) up to the time of contacting the strain control plate, see Fig 6. One explanation for the equalizing of the force between the top and bottom of the sample could be the high fluid content in the tissue. Nonetheless, the result is surprising since it indicates that the tissue is behaving similar to a fully confined fluid in this respect. These equilibrated force measurements indicate that the inertia force associated with accelerating portions of the tissue during the test are negligible.

The ultimate goal was to measure stress-stretch relationships for the tissue at strain rates relevant to automotive impacts. Clearly, given the complex deformation behaviour observed, this can only be done

in an average sense and more detailed inverse finite element modelling would be necessary to attempt to extract truly local material properties. Nonetheless, the engineering stress evaluations presented in Fig 10 & 11 do provide useful information on the dynamic deformation behaviour of fresh porcine skeletal muscle tissue in both the fibre and cross-fibre direction at automotive impact rates. The cross-fibre stress-stretch data presented in Fig. 10 are averages of four tests at 11,600%/s, twelve tests at 22,000%/s and five tests at 37,800%/s and the standard deviations are also shown. The fibre direction data are averages of five repeated tests at 22,000%/s and five tests at 37,800%/s and again the standard deviations are shown. The results show nonlinear stress-strain relationships as well as clear stiffening with increasing strain rate, which is qualitatively similar to results from lower rate testing [4, 8, 10, 14, 15]. The stress at 30% compression was approximately 9 times higher for the strain rate of 37800%/s compared to 11600%/s, which is qualitatively similar to observations at other strain rates [4, 15, 20]. The cross-fibre direction was observed to be stiffer than the fibre response at a given strain rate (compare Fig. 10 to Fig. 11), similar to previous observations at different rates, [4, 8, 15] but the differences observed here between the fibre and cross-fibre direction responses were small.

Direct comparison with the frozen and then thawed human tests by Chawla et al [14] is difficult as slightly different strain rates were used, but a broad comparison shows that the stress at a stretch of 0.7 for the cross-fibre direction tests at both 11,600%/s and at 22,000%/s was about two to three times more compliant for the current tests than for the results of Chawla et al. This may be due to the effects of rigor mortis on their results, as discussed earlier, but may also reflect other differences. As Chawla et al did not test in the fibre direction, it is not possible to compare those results, and they did not comment on fluid expulsion in their testing.

In order to assess the evolution of stress with strain rate, Van Loocke [7] used a stress normalisation method to compare different experimental data obtained from different protocols and this is applied again here. For each experimental protocol, the stress value from the lowest strain rate was taken as a reference and the ratios between this value and values obtained at higher rates were calculated. The resulting stress ratios were then combined to show the increase in stress from a reference strain rate of 0.05%s-1 (which now gives a ratio of 1), see Fig 13. A continuous evolution by comparison with the ramp and cyclic tests reported in the literature [3, 4, 7, 15] is evident, but the results presented here are stiffer response than the split Hopkinson bar tests results observed by Song et al [8].

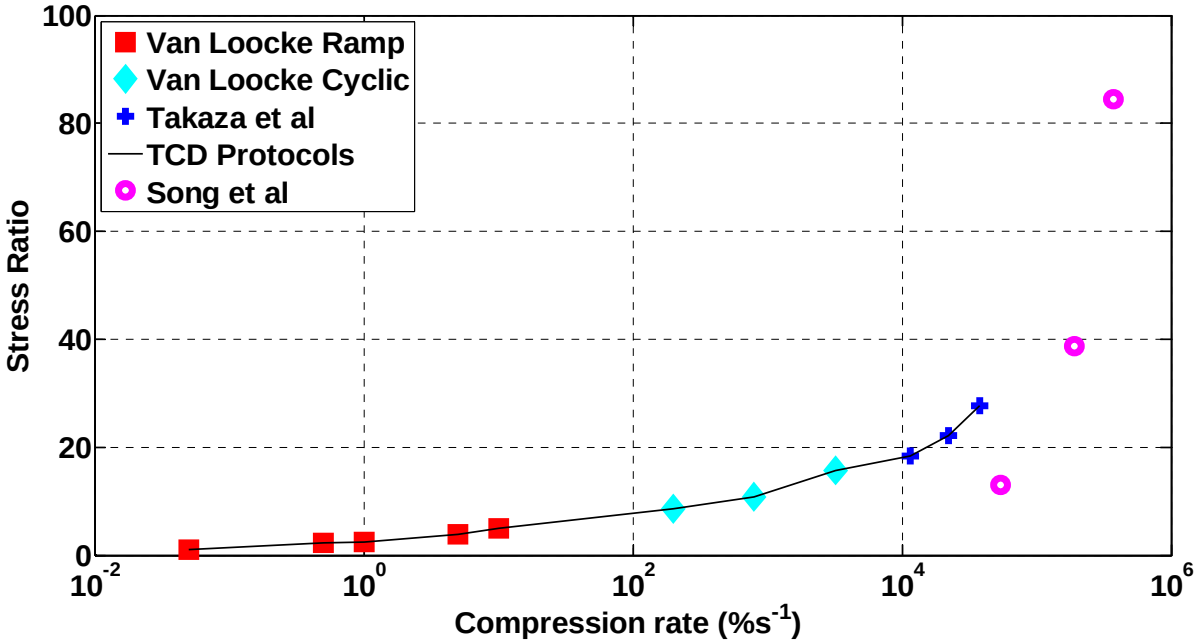

Figure 11. Relative increase in stress with compression rate for skeletal muscle tissue. Values calculated from tests performed by [7] and Song et al and this experiment

Overall, in this paper we have provided new three-dimensional data on the impact response of fresh passive porcine skeletal muscle tissue at rates relevant to automotive impacts. We have tested both the fibre and the cross-fibre direction and we have tested on fresh porcine tissue prior to the onset of

rigor mortis. Furthermore, we have used the same tissue preparation and testing protocol as in our earlier quasi-static testing work, and this has allowed calculation of the evolution of stress increase with compression rate in a way that was not previously possible. Finally, we have attempted to characterize the strain variation within the samples and the fluid behaviour within the tissue during the impact process. To the best of our knowledge, this has not been reported before. However, it may be premature to use this data in finite element models as the work presented here is experimental deformation work and an appropriate material model would be required prior to implementation in global human body models.

V. CONCLUSIONS

Freshly slaughtered cuboidal shaped porcine muscle samples were compressively impact loaded using a custom-designed drop tower testing rig. At a stretch ratio of 0.7, the following engineering stress responses magnitudes were observed: 5.95kPa ±0.6kPa, 25.88kPa ±5.3kPa and 43.68kPa (±1.4kPa) at strain rates of 11,600%/s, 22,000%/s and 37,800%/s respectively for load applied in the cross-fibre direction. For loading applied in the fibre direction, the following engineering stress responses magnitudes were observed: 22.03kPa ±1.5kPa and 37.06kPa ±3.0kPa at strain rates of 22,000%/s and 37,800%/s respectively. A compressive stress wave was observed to propagate downwards and muscle fluids were ejected at the front of the wave resulting in an average sample mass loss of 8%. For the strain rates tested, which are relevant to automotive impact cases, skeletal muscle displays a nonlinear stress stretch relationship as well as a clear rate dependency.

VI. ACKNOWLEDGEMENT

The authors would like to acknowledge Paul Normoyle for the Labview data acquisition help he contributed and Peter O'Reilly for the technical help and Mick Reilly for his help in building the rig.

VII. REFERENCES

[1] Chomentowski P, Coen PM, Radikova´ Z, Goodpaster, BH, Toledo, FGS, Skeletal muscle mitochondria in insulin resistance- differences in intermyofibrillar versus subsarcolemmal subpopulations and relationship to metabolic flexibility. *J. Clin. Endocrinol.* Metab, 96(2), p. 494-503, 2011.

[2] Salem RO, Laposata M, Rajenram R, Cluette-Brown JE, Preedy VR, The total body mass of fatty acid ethyl esters in skeletal muscles following ethanol exposure exceeds that found in the liver and the heart. *Alcohol & Alcoholism* ,41(6), p. 598-603, 2006.

[3] Van Loocke M, Simms CK, and Lyons CG, Viscoelastic properties of passive skeletal muscle in compression--Cyclic behaviour. *Journal of Biomechanics*, 42(8): p. 1038-1048, 2009.

[4] Van Loocke M, Simms CK, and Lyons CG, A validated model of passive muscle in compression. *Journal of biomechanics*, 39, p. 2999-3009, 2006.

[5] Vignos JPJ. and Lefkowitz M, A biochemical study of certain skeletal muscle constituents in human progressive muscular dystrophy. *The Journal of Clinical Investigation*, 38, p. 873-881, 1959.

[6] Nie X, Cheng Jen-I, Chen W W, Weerasooriya T, Dynamic tensile response of porcine muscle. *J. Appl. Mech*.,78(2), p. 021009 (1-5), 2011.

[7] Van Loocke, M., Passive mechanical properties of skeletal muscles in compression, in Mechanical & Bioengineering Department, Trinity College Dublin: Dublin, 2007.

[8] Song B, Chen W, Ge Y Weerasooriya T, Dynamic and quasi-static compressive response of porcine muscle. *Journal of Biomechanics*, 40(13), p. 2999-3005, 2007

[9] Sacks MS, Biaxial Mechanical Evaluation of Planar Biological Materials. *Journal of Elasticity*, 61: p. 199-246, 2000.

[10] Van Sligtenhorst C, Cronin DS, Brodland GW, High strain rate compressive properties of bovine muscle tissue determined using a split Hopkinson bar apparatus. *Journal of Biomechanics*, 39(10), p. 1852-1858, 2000.

[11] Morrow DA, Donahue TLH, Odegard GM, Kaufman, K. R. Transversely isotropic tensile material properties of skeletal muscle tissue. *Journal of the Mechanical Behavior of Biomedical Materials*, 3(1), p. 124-129. 2010.
[12] Dhaliwal ST, Beillas P, Chou CC, Prasad P,Yang HK, King, I A, Structural response of the lower leg muscles in compression: A low impact energy study employing volunteers, cadavers and the hybrid III. *Stapp car crash Journal*, 46, p. 229-243, 2002.
[13] Muggenthaler H, von Merten K, Peldshus S, Holley S, Adamec J, Praxl N, Graw M, Experimental test for the validation of active numerial human models. *Forensic Science International*, 177, p. 184-191, 2008.
[14] Chawla A, Mukherjee S. Karthikeyan B, Characterisation of human passive muscles for imapct loads using genetic algorithm and inverse finite element methods. *Biomech Model Mechanobiol*, 8, p. 67-76. 2009
[15] Van Loocke M, Lyons CG, Simms CK, Viscoelastic properties of passive skeletal muscle in compression: Stress-relaxation behaviour and constitutive modelling. *Journal of Biomechanics*, 41(7), p. 1555-1566, 2008.
[16] McElhaney JH, Dynamic response of bone and muscle tissue. *Journal of Appl. Physio*,. 21(4): p. 1231-1236, 1966
[17] Takaza M, Moerman KM, Gindre J, Simms CK, The anisotropic mechanical behaviour of passive skeletal muscle tissue subjected to large tensile strain. *Journal of the Mechanical Behavior of Biomedical*, In Revision.
[18] Jolliffe KH, Heymann FJ, Scriven RA, Brunton JH, Field JE, Broom T, Langbein G, Smith A, Benjamin TB, Atkins AG, Carpenter SK, Popple RG, Jenkins DC, Shal'nev KK, Thomas LA, Tomalin PF, Tabor D, Edeleanu C, The Application of Dislocation Etching Techniques to the Study of Liquid Impacts [and Discussion]. *JSTOR*, 260(1110), p. 101-120, 1966.
[19] Arfken AG, Griffing FD, Kelly CD Priest J, University Physics, Chicago: Harcourt Brace Jovanovich 1989.
[20] Zheng Y, Mak AFT, Lue B, Objective assement of limb tissue elasticity; Development of a manual indentation procedure, *Journal of Rehabilitation Research and Development*, 36, p. 2. 1999.